Phonon anomalies near the magnetostructural transition in Li_2RuO_3: Raman spectroscopy and density functional theory studies

Yuri S. Ponosov,[1,2] Evgenia V. Komleva,[1] and Sergey V. Streltsov[1,2]
[1]*M.N. Mikheev Institute of Metal Physics, S. Kovalevskaya Street 18, 620137 Ekaterinburg, Russia*
[2]*Ural Federal University, Mira Street 19, 620002 Ekaterinburg, Russia*

(Received 1 August 2019; revised manuscript received 17 September 2019; published 21 October 2019)

Raman spectroscopy is used to control the kinetics of the magnetostructural transition in Li_2RuO_3 crystals from the low-temperature dimerized phase ($P2_1/m$) to the high-temperature phase ($C2/m$) at $T_c \sim 550$ K accompanied by the destruction of the spin singlets on the Ru-Ru bonds. The theoretical group analysis and the results of the density functional theory calculations of the lattice dynamics were used to identify phonon modes that are sensitive to the transition. The observed anomalies in the behavior of the self-energies of such phonons near T_c suggest their connection either with possible dynamic disordering of Ru atomic positions or with spin-phonon interaction.

DOI: 10.1103/PhysRevB.100.134310

I. INTRODUCTION

The family of honeycomb-lattice ruthenates reveals a number of unique intriguing phenomena. Recently, it was discovered that the honeycomb-lattice compound Li_2RuO_3 exhibits an unusual phase transition at $T_c \sim 540$–560 K. The crystal structure of Li_2RuO_3 consists of honeycomb layers of RuO_6 and LiO_6 edge-sharing octahedra, which alternate with Li layers along the c direction. Below T_c two of the six Ru-Ru bonds in the honeycomb hexagon become substantially shorter ($\sim$18%) than the others, forming static Ru-Ru dimers. Because of this dimerization, the high-temperature structure with a nearly ideal honeycomb lattice, on average having the space group $C2/m$, is transformed to a less symmetric structure with a distorted honeycomb lattice (space group $P2_1/m$) below T_c [1,2]. This dimer transition is accompanied by a strong decrease of the magnetic susceptibility.

It was argued in Ref. [3] that physical properties of this system are controlled by orbital physics when a specific orbital pattern induces spontaneous dimerization and results in the spin-singlet ground state. The authors suggested that the magnetoelastic interaction with Li ions is important in order to remove orbital degeneracy and obtain a dimerized superstructure in the form of the armchair pattern observed in the experiment. Indeed, electronic structure calculations showed the existence of a rather fine structure near the Fermi level, corresponding to molecular orbitals, formed by Ru t_{2g} orbitals (with some admixture of O $2p$ states), in the low-temperature phase, which are smeared at high temperatures [2,4]. A high-energy x-ray diffraction experiment using a pair distribution function analysis revealed that the dimers exist even above T_c, but the positions of the dimers change dynamically: they start to flow [5]. Nuclear magnetic resonance measurements also revealed some activation processes associated with the motion of the Ru-Ru dimers [6].

It has been demonstrated that disorder introduced by either synthesis conditions or substitution effects sensitively affects the coherence of dimerization, which is reflected in the lattice parameters as well as in the sharpness of magnetic transition [7–10]. One might expect that lattice distortions induced by lattice vibrations (especially ruthenium atoms) should also affect the coherence of the dimer superstructure, which can be reflected in changes in phonon frequencies and widths. However, the supposed strong influence of lattice vibrations on the real superstructure has not yet been studied experimentally by direct monitoring of the phonon spectrum during the magnetostructural transition. This can be done using Raman spectroscopy, which is also sensitive to the short-range order, which, as previously assumed, is maintained even at temperatures significantly higher than T_c. In our work, *in situ* studies of the phonon spectrum in a wide temperature range on single-crystal samples were performed using this experimental technique, as well as first-principle calculations of the phonon spectrum.

II. EXPERIMENTAL AND CALCULATION DETAILS

Raman experiments were carried out on freshly cleaved surfaces of compacted disks of Li_2RuO_3 polycrystalline powder. We used the same samples on which experiments [4,6] were previously performed. These samples of Li_2RuO_3 were synthesized using a solid-state reaction method as described in [4,6]. Measurements of x-ray diffraction and magnetization confirmed the high quality of our samples, showing clear signs of the phase transition at around 560 K.

Polarized Raman measurements in the temperature range of 80 to 840 K were performed in backscattering geometry using an RM1000 Renishaw microspectrometer equipped with a 532-nm solid-state laser and 633-nm helium-neon laser. The respective Linkam stage was used for temperature variation. Most of the measurements were done on hexagonal microcrystals (inset in Fig. 1), that is, on an ab (XY) plane, and the long axis is assumed to be the b axis. Polarization measurements on many such crystals gave repetitive spectra

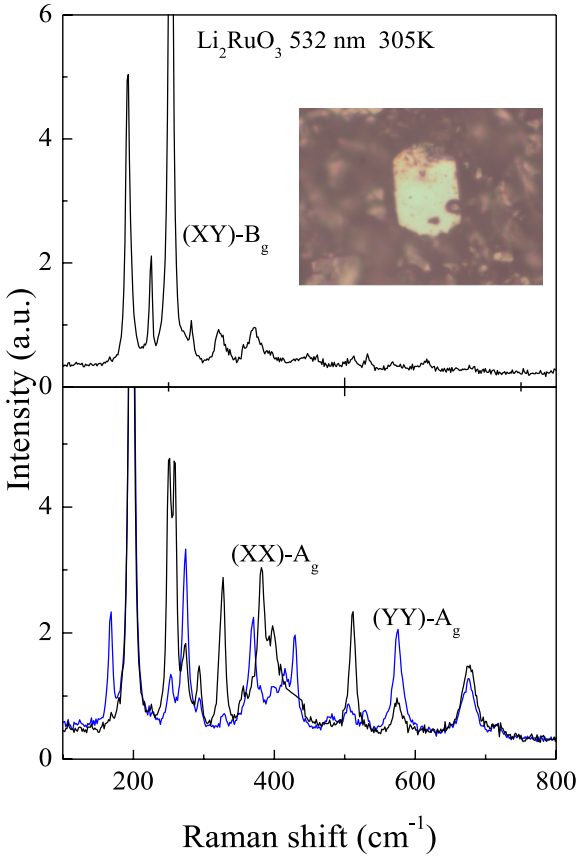

FIG. 1. Experimental phonon Raman spectra of Li_2RuO_3 measured at 300 K in different polarization geometries. Excitation is 532 nm. Inset: micrograph of the crystallite in the used sample, as seen in an optical microscope.

for the used polarizations. Measurements on thin rectangular crystals (YZ orientation) confirmed results obtained in measurements on hexagonal-shaped crystals. The laser beam was focused (5 μm in diameter) on such microcrystals up to 30 μm in size with very low power (up to 0.1 mW) to avoid local heating of the crystals.

Calculations of the phonon spectra were performed using the frozen-phonon method implemented in PHONOPY [11], and the electronic structure was obtained with the Vienna *Ab initio* Simulation Package (VASP) [12]. For both high- and low-temperature phases $2 \times 2 \times 2$ supercells were used. We applied $8 \times 8 \times 8$ and $8 \times 4 \times 8$ k meshes for $C2/m$ and $P2_1/m$ structures, respectively. For enlarged supercells we proportionally reduced k-mesh densities. The plane-wave cutoff energy was chosen to be 500 eV. The density functional theory (DFT) iterations were repeated until the total energy change was more than 10^{-7} eV between electronic steps and more than 10^{-6} eV between ionic steps.

III. RESULTS AND DISCUSSION

A. Phonon Raman spectra of Li_2RuO_3

First of all, we present results of group theoretical analysis of vibrational spectra of both low- and high-temperature phases of Li_2RuO_3 in order to determine the number and symmetry of modes, which are expected to contribute to Raman scattering spectra.

The low-temperature structure is characterized by the $P2_1/m$ space group (unique axis b), and there are 24 atoms in a unit cell. Ru-Ru dimers are ordered in the armchair structure mentioned above. The following modes should be observed in the Γ point in this structure:

$$\Gamma = 20A_g + 16B_g + 20B_u + 16A_u, \quad (1)$$

where A_g and B_g modes are Raman active, while B_u and A_u are infrared (IR) active. The high-temperature structure (i.e., above $T_c \sim 560$ K) is characterized on average by the $C2/m$ space group. There are 12 atoms in a primitive cell [1], and one expects 36 phonon modes in the Γ point:

$$\Gamma = 7A_g + 8B_g + 13B_u + 8A_u. \quad (2)$$

The first two terms correspond to Raman active modes, while the last two can be observed only using IR spectroscopy.

Figure 1 shows the polarized Raman spectra of Li_2RuO_3 measured in the low-temperature phase at 300 K in the in-plane XX, YY, and XY polarizations of incident and scattered light. The XY polarization probes the B_g symmetry, while YY and XX polarizations probe the A_g symmetry channel. Despite the large number of allowed lines, all 20 A_g phonons are well resolved in the spectra with polarizations YY, XX, and ZZ (Figs. 1–4), with the same phonon lines having different intensities for different components of the Raman tensor. In the XY polarization geometry (B_g) the number of lines (10) is less than that predicted by the selection rules (16), and the most intense are located in the low-frequency region. The spectra obtained make it possible to assert that the experiment was performed on untwinned single crystals. A good benchmark is the two B_g lines at 225 and 253 cm^{-1} in spectra with XY polarizations, which are absent in the XX and YY spectra. Their appearance in these geometries in measurements on some hexagonal-shaped crystals indicates that these crystals were twinned.

The frequencies of the phonon lines observed in the low-temperature $P2_1/m$ phase are presented in Table I together with the calculated data. Although the inability to observe all Raman active B_g modes makes the frequency assignment of some of them ambiguous, in general, the calculation performed shows good agreement with the experimental frequencies in the low and medium energies, while the correspondence is somewhat worse in the high-frequency range. We have to note that calculations produced one B_u mode with slightly negative frequencies. However, as seen in Table I, for the modes in the frequency interval of interest (above 160 cm^{-1}) there seems to be reasonable agreement between calculated and experimental data (the standard deviation of experimental frequencies from calculated ones is only ~8%), which justifies the presented comparative analysis.

In order to study the structural phase transition in Li_2RuO_3 in detail, the Raman spectra were measured between 80 and 860 K. Most temperature measurements were performed in the YY and ZZ polarization geometries. With increasing temperature, the frequencies of all lines in the spectra decrease, and their widths increase (Figs. 2–4). In addition, the intensity of the background on which the phonon peaks are superimposed increases by 5–10 times in the low-frequency

TABLE I. Calculated and experimentally found at 300 K frequencies (in cm^{-1}) of Raman active modes for the LT phase (space group: $P2_1/m$) of Li_2RuO_3 with respect to the polarization geometry in which they are observed. Corresponding irreducible representations are also shown.

		Frequency			
			Experiment		
No.	Symmetry	Theory	(XX-A_g)	(YY-A_g)	(XY-B_g)
1	A_g	677	715	715	
2	B_g	657			615
3	A_g	551	675	675	
4	A_g	523	601		
5	B_g	506			533
6	A_g	504	575	575	
7	B_g	501		529	
9	B_g	487			445
10	A_g	466	512		
11	B_g	460			
12	A_g	449		480	
13	B_g	433			
14	A_g	419		430	
15	B_g	418			372
16	A_g	408		415	
17	A_g	384	399	399	
18	A_g	366	382		
19	A_g	351	369	369	
20	B_g	344			
21	B_g	340			
22	B_g	331			323
23	A_g	321	356		
24	A_g	316	327	327	
25	B_g	309			282
26	A_g	283	293		
27	B_g	272			
28	A_g	271		274	
29	B_g	254			253
30	B_g	248			
31	A_g	245	259		
32	A_g	226	251		
33	B_g	215			225
34	A_g	199	198	198	
35	B_g	173			192
36	A_g	171		168	

region at the highest temperatures for the in-plane polarization geometries but does not change much for the ZZ geometry. It is likely that this background has an electronic nature. This issue will be the subject of a separate publication.

As the temperature approaches T_c from below, the intensity of certain lines significantly reduces, and they completely disappear at $T \geqslant 580$ K (Figs. 2–4). High-frequency lines measured in the ZZ geometry only slightly change the intensity with increasing temperature (Fig. 3). The number of lines in the high-temperature phase is quite difficult to calculate because of their large width and possible overlap, as well as the ambiguous subtraction of the background. An attempt to decompose the observed YY spectrum at 830 K (Fig. 2) gives seven lines, a number equal to the expected seven A_g peaks for the averaged $C2/m$ structure of the high-temperature

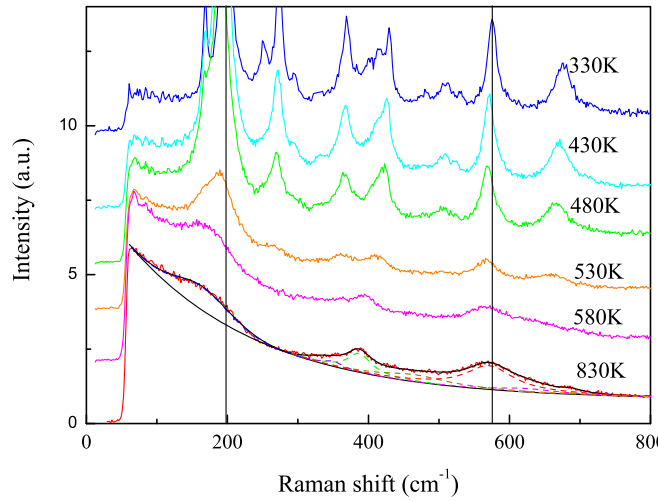

FIG. 2. Experimental phonon Raman spectra of Li_2RuO_3 measured in YY polarization geometry at different temperatures. Excitation is 532 nm. Decomposition of the spectrum measured at 830 K into phonon components and estimated background are shown for the bottom curve. Vertical lines indicate the frequency of individual vibrations at low temperatures. Low-frequency points before the filter cutoff (~60 cm^{-1}) show the spectrum zero level shifted.

phase. They are located at 165, 338, 386, 483, 570, 625, and 690 cm^{-1}. The positions of the A_g peaks for $T \geqslant T_c$ measured in the YY and XX geometries practically coincide. Broad features near 190, 400, and 660 cm^{-1} are observed for the B_g (XY) spectra (see Fig. 4).

For the quantitative analysis of phonon parameters in Li_2RuO_3 individual phonon lines were fitted by Lorentz profiles (after background subtraction). Three high-frequency lines dominate the ZZ spectrum, which made it possible to obtain the temperature dependences of their self-energies more accurately than in the YY geometry. The resulting

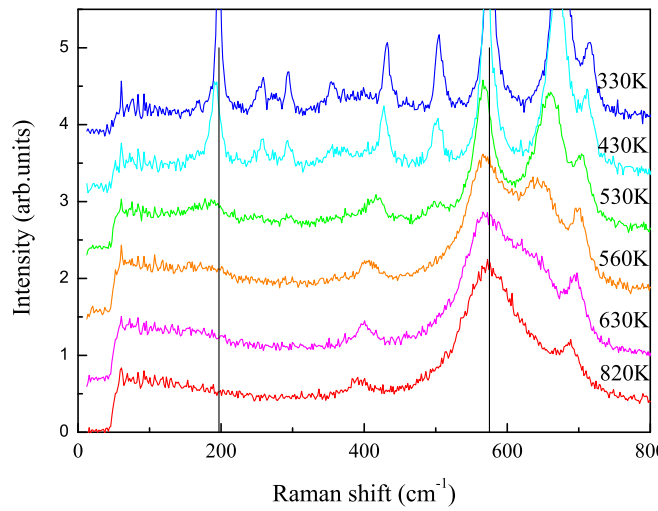

FIG. 3. Experimental phonon Raman spectra of Li_2RuO_3 measured in the ZZ polarization geometry at different temperatures. Excitation is 532 nm. Vertical lines indicate the frequency of individual vibrations at low temperatures. Low-frequency points before the filter cutoff (~60 cm^{-1}) show the spectrum zero level.

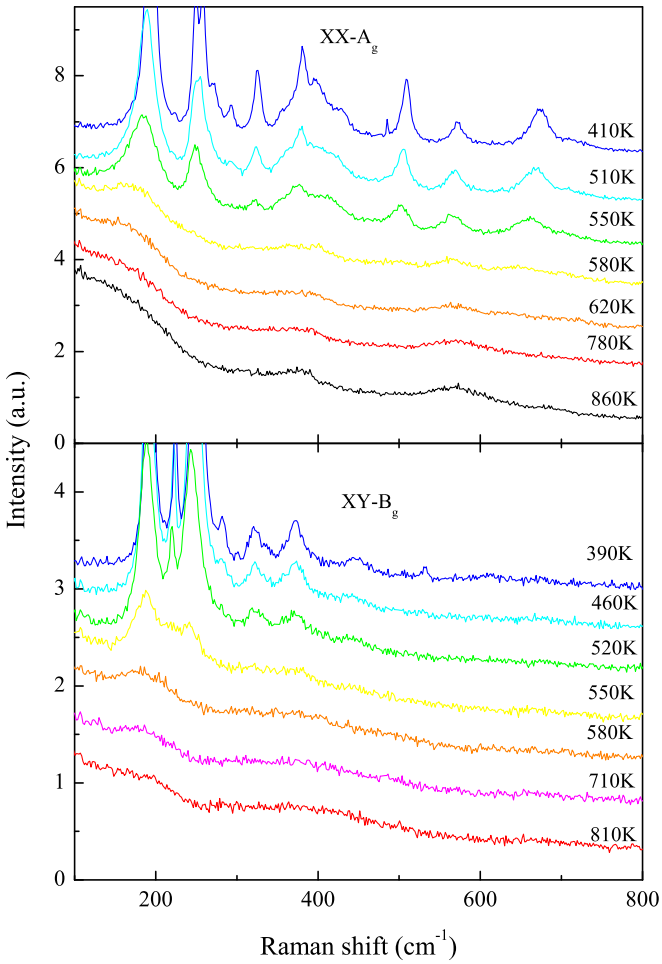

FIG. 4. Experimental phonon Raman spectra of Li_2RuO_3 measured in XX and XY polarization geometries at different temperatures. Excitation is 532 nm.

frequencies and full widths at half maximum (FWHM) for four A_g modes, 198, 575, 675, and 715 cm^{-1}, are plotted in Fig. 5 as a function of temperature. As can be seen, the phonon frequencies soften when approaching the transition temperature, and the linewidths increase, which can be explained by anharmonic effects. The same tendency is characteristic for B_g vibrations (see Fig. 6). In the simplest form, the temperature behavior of phonon self-energies is described by formulas that assume the decay of an optical phonon into two phonons of half the frequency with opposite wave vectors [13]. We showed such anharmonic contributions to the frequency and linewidth for four A_g Raman active phonons in Fig. 5. The contributions to the phonon frequencies are somewhat overestimated since we were not able to estimate the contributions of thermal expansion due to the lack of complete temperature data and the mode Grüneisen coefficients necessary for such an estimate. Nevertheless, the behavior of frequencies in the low-temperature phase is rather well reproduced when such contributions are taken into account. The frequencies of the lines at 198, 675, and 715 cm^{-1} show a noticeable softening near the transition, while the frequencies of the A_g line at 575 cm^{-1} and the B_g line at 192 cm^{-1} (Fig. 6) soften over the entire temperature range below the transition and then show an anomalous hardening above T_c. The widths of all

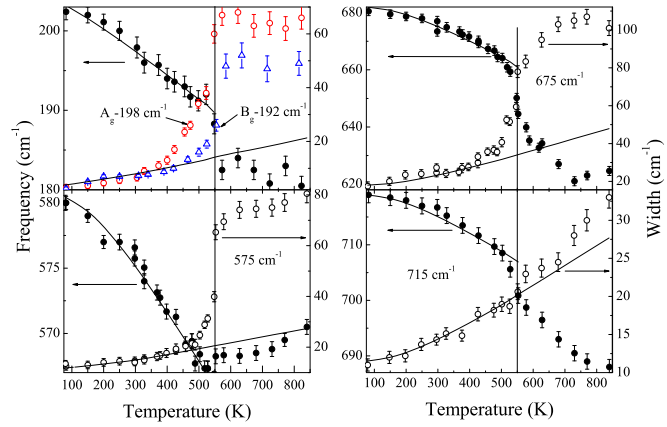

FIG. 5. Temperature dependences of the frequency (solid circles) and full width at half maximum (open circles) of the 198, 575, 675, and 715 cm^{-1} modes. The linewidth of the B_g mode at 192 cm^{-1} is also shown. The vertical bars indicate the structural transition temperatures. The solid lines are the frequency and linewidth fits to the anharmonic model [13].

lines grow abnormally at the transition, with the exception of the line at 715 cm^{-1}, which shows the smallest and gradual growth over the entire temperature range. The phonon at 430 cm^{-1} also shows noticeable softening and broadening near the transition, although it is difficult to extract exact figures. The results obtained assume that all the lines of the high-temperature phase are successors of the lines of the low-temperature phase.

The obtained broadening of the phonon widths at $T \geqslant T_c$ significantly exceeds the contribution of anharmonicity,

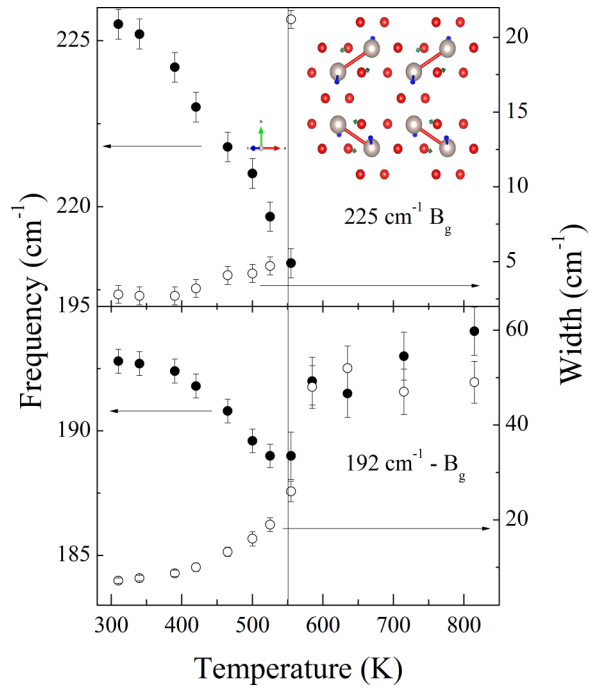

FIG. 6. Temperature dependences of the frequency (solid circles) and full width at half maximum (open circles) of two B_g modes at 192 and 225 cm^{-1}. The inset shows the vibrational pattern of the 225 cm^{-1} B_g mode.

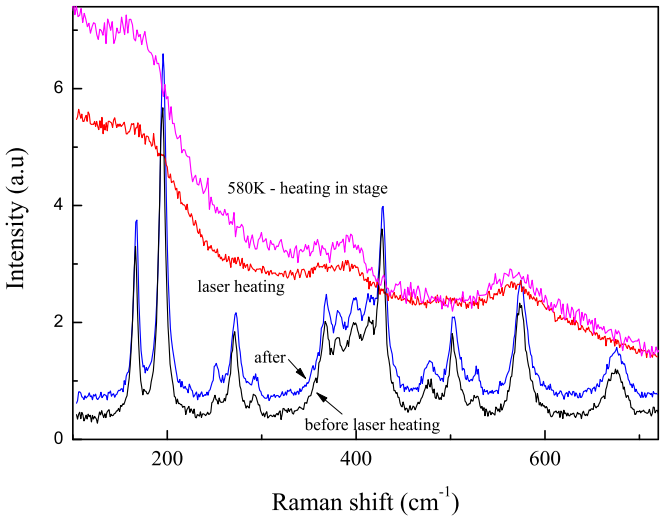

FIG. 7. Raman spectra of Li_2RuO_3 measured at 330 and 580 K using low incident laser power and spectra measured with high laser power and after a quick power release. Excitation is 633 nm.

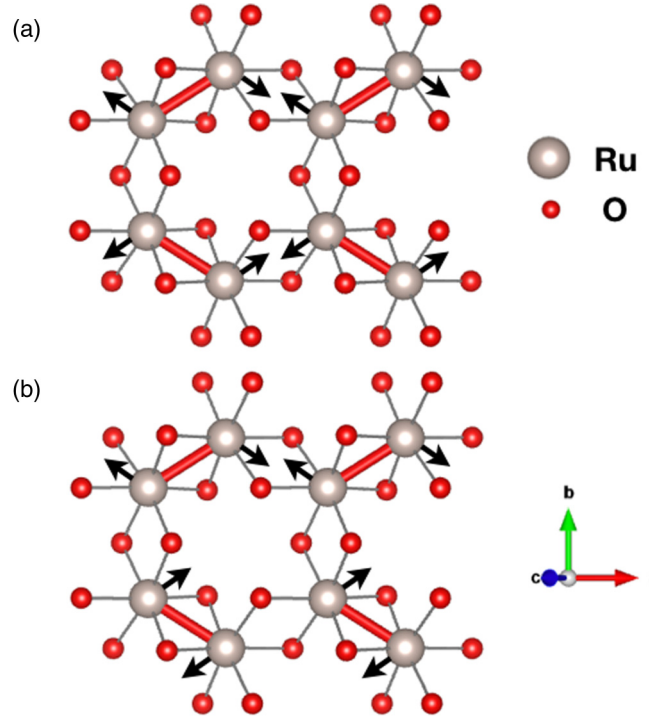

FIG. 8. Vibrational pattern of the (a) 198 cm^{-1}-A_g and (b) 192 cm^{-1}-B_g modes in the low-temperature phase. Red balls are oxygen atoms. Ru-Ru dimers are depicted in red.

estimated in a simple model [13], as shown in Fig. 5 for 192 cm^{-1} (B_g) and 198, 575, and 675 cm^{-1} (all A_g) modes while the linewidth of the 715 cm^{-1} (A_g) phonon implies that the main broadening is due to the anharmonic contribution. The observed increase in the width of the lines may indicate that the transition is an order-disorder transition, with a dynamic disorder of the positions of the ruthenium atoms in the high-temperature phase. We attempted to rapidly cool the sample from high temperatures using local heating with high incident 633-nm laser power (15×). Figure 7 shows that with such local heating the shape of the phonon spectrum is very close to the shape of the spectrum of the high-temperature phase obtained by heating on a stage using a low laser power. Subsequent measurement after a quick power release captures the original spectrum obtained with low laser power at 330 K. In this way, this gives arguments in favor of dynamic rather than static disorder in the high-temperature phase. However, it should be noted that, although the Raman experiment is sensitive to the local environment in the sample, i.e., to the short-range order, it does not provide direct evidence of the existence of dimers in the high-temperature phase, as suggested in [5]. A significant decrease in the number of lines in the high-temperature phase is more likely consistent with the structure of $C2/m$, with significant fluctuations in the positions of the atoms of Ru.

B. Discussion

Thus, the changes observed in the phonon spectra confirm that at 540–560 K a structural transition from the $P2_1/m$ phase to the $C2/m$ phase occurs. At the same time, some lines demonstrate a rather drastic softening of their frequencies, while the energies of others change continuously. This may indicate that the nature of the transition is not straightforward and combines features of both the first and second orders. The widths of all phonon lines increase significantly with increasing temperature. So the linewidth at 198 cm^{-1} starts to grow already from room temperature, increases by an order of magnitude before T_c, and then finally jumps to the maximum in the high-temperature phase. The change in the damping of high-frequency phonons occurs closer to T_c. Estimates show that such a strong growth of phonon damping cannot be explained only by the phonon-phonon interactions with the exception of the phonon at 715 cm^{-1}.

The pattern of the displacements of Ru atoms in the A_g mode at 198 cm^{-1} is such that the dimers in adjacent chains running along the a axis rotate in different directions in the ab plane [Fig. 8(a)]. In this case, the angle between the dimers in the neighboring chains varies, although the dimers remain parallel in each chain. Very similar displacements of Ru atoms in chains are calculated for B_g vibration at 192 cm^{-1} [Fig. 8(b)]. However, here the rotation of the dimers in each chain occurs in one direction, and the angle between the dimers in the adjacent chains is maintained. The frequencies of these modes are close, so the anharmonic contributions to the linewidth should also be the same, which is confirmed by the observed low-temperature broadenings of these lines. The substantial difference in the phonon widths in the low-temperature phase at $T \geqslant 300$ K for these two modes (Fig. 5) implies a strong sensitivity of the A_g mode to the dynamic disorder, which follows logically from the nature of atomic displacements. The displacement of Ru atoms in the direction perpendicular to the ab plane weakly affects the phonon damping, which can be seen in the example of the B_g mode at 225 cm^{-1}, which, up to the transition, has an anomalously narrow linewidth (Fig. 6). The transition to the high-temperature phase leads to a sharp change in the widths of the lines of most phonon lines, with the exception of the highest-frequency A_g mode at 715 cm^{-1}. The calculated displacements of the Ru atoms

for this mode are very small for both the low-temperature and high-temperature phases. This would seem to correlate with small temperature variations in the linewidth of this mode. However, a significant increase in the widths of the lines of other high-frequency A_g modes at 575 and 675 cm^{-1}, also mainly due to the motions of oxygen atoms, raises the question of the reason for this behavior. As we saw in the example of the 198 cm^{-1} mode, the dynamic disorder in the arrangement of dimers significantly affects the width of the phonon lines already in the low-temperature phase. The existence of such a disorder in the high-temperature phase in the form of floating dimers, assumed in [5], can lead to observable effects in the case of a strong sensitivity of certain oxygen modes to dynamic fluctuations of the positions of Ru atoms (i.e., significant variations of the interatomic force constants of Ru-O).

On the other hand, displacements of Ru atoms strongly affect exchange coupling in Ru-Ru dimers, which may result in the development of (singlet) spin fluctuations with its further sharp increase in the high-temperature phase. In this scenario, at least part of the growing damping of the phonon mode at 198 cm^{-1} below transition can be explained by the spin-phonon interaction. Perhaps this explains the unusual two-step growth of its linewidth. The assumption of the contribution of the spin-phonon interaction to the linewidths of high-frequency oxygen modes probably requires the existence of an exchange interaction Ru-O-Ru. The observation of an electronic background that grows with increasing temperature may be associated with the manifestation of such an interaction and requires detailed study.

Thus, in a related compound with the ruthenium honeycomb lattice, $SrRu_2O_6$, that does not have dimers, a significant increase in phonon damping of high-frequency oxygen modes was also observed in a wide temperature range near $T_N \sim$ 560 K along with an increase in the magnetic susceptibility [14]. α-$MoCl_3$, possessing a honeycomb lattice of molybdenum layers, also reveals a magnetostructural transition near 585 K without a change in the crystal structure, but with a significant rearrangement of the structure of dimers. In this compound, the Raman spectrum also detects a significant increase in the width of the lines near the transition [15]. The spin-lattice coupling was discussed as a source of the large phonon linewidths found in Raman scattering experiments on iridates with square-lattice networks of iridium ions, Sr_2IrO_4 and $Sr_3Ir_2O_7$ [16].

IV. CONCLUSIONS

In summary, we investigated the phonon spectra of Li_2RuO_3 both experimentally using Raman scattering on single crystals in a wide temperature range and theoretically within the DFT lattice dynamics calculations. The change in the number of lines near 540–560 K confirms that a structural transition from the $P2_1/m$ to $C2/m$ phase occurs, combining features of both the first and second orders. An attempt to relate the observed anomalous growth of the widths of most phonon modes near the transition to the atomic displacement pattern for these modes showed that distortion of the dimer superstructure during the vibrations of Ru atoms leads to a significant increase in phonon damping for such modes already in the low-temperature phase. This suggests that an additional contribution to the width of such lines is associated with the spin-phonon interaction, or more specifically, it arises from the development of spin fluctuations during the distortion of the dimerized superstructure. If the high-temperature phase is a valence bond liquid, where dimers are preserved but dynamically disordered [5], the anomalously large width of phonon lines in the high-temperature phase can be explained by purely structural disorder. However, the above-mentioned fact of additional phonon damping in the low-temperature phase raises the question of the contribution of spin-phonon effects to the widths of the lines not only of Ru-Ru vibrations but also of high-frequency modes associated with the motion of oxygen atoms.

ACKNOWLEDGMENTS

The authors are grateful to J. G. Park for providing the samples, V. I. Voronin and D. V. Privalova for the attestation of the samples, and D. A. Zamyatin for his assistance with low-temperature measurements in CCU "Geoanalyst," IGG, UB RAS. E.V.K. and S.V.S. thank N.N. Krasovskii Institute of Mathematics and Mechanics UB RAS for providing facilities for the calculations. The research was carried out within the state assignment of the Ministry of Science and Higher Education of the Russian Federation (theme "Electron" No. AAAA-A18-118020190098-5, and theme "Quantum" No. AAAA-A18-118020190095-4) and Contract No. 02.A03.21.0006, and was supported in part by RFBR (Grant No. 19-52-18008) and by the Ural branch of RAS (Grant No. 18-10-2-37).

[1] Y. Miura, Y. Yasui, M. Sato, N. Igawa, and K. Kakurai, J. Phys. Soc. Jpn. **76**, 033705 (2007).
[2] Y. Miura, M. Sato, Y. Yamakawa, T. Habaguchi, and Y. Ōno, J. Phys. Soc. Jpn. **78**, 094706 (2009).
[3] G. Jackeli and D. I. Khomskii, Phys. Rev. Lett. **100**, 147203 (2008).
[4] Z. V. Pchelkina, A. L. Pitman, A. Moewes, E. Z. Kurmaev, T.-Y. Tan, D. C. Peets, J.-G. Park, and S. V. Streltsov, Phys. Rev. B **91**, 115138 (2015).
[5] S. A. J. Kimber, I. I. Mazin, J. Shen, H. O. Jeschke, S. V. Streltsov, D. N. Argyriou, R. Valentí, and D. I. Khomskii, Phys. Rev. B **89**, 081408(R) (2014).
[6] I. Yu. Arapova, A. L. Buzlukov, A. Yu. Germov, K. N. Mikhalev, T.-Y. Tan, J.-G. Park, and S. V. Streltsov, JETP Lett. **105**, 375 (2017).
[7] M.-P. Jimenez-Segura, A. Ikeda, S. Yonezawa, and Y. Maeno, Phys. Rev. B **93**, 075133 (2016).
[8] H. Lei, W.-G. Yin, Z. Zhong, and H. Hosono, Phys. Rev. B **89**, 020409(R) (2014).
[9] I. Terasaki, S. Abe, Y. Yasui, R. Okazaki, and H. Taniguchi, J. Mater. Chem. C **3**, 10430 (2015).
[10] K. Mehlawat and Y. Singh, Phys. Rev. B **95**, 075105 (2017).
[11] A. Togo and I. Tanaka, Scr. Mater. **108**, 1 (2015).

[12] G. Kresse and J. Hafner, Phys. Rev. B **47**, 558 (1993).
[13] P. G. Klemens, Phys. Rev. **148**, 845 (1966).
[14] Y. S. Ponosov, E. V. Komleva, D. A. Zamyatin, R. I. Walton, and S. V. Streltsov, Phys. Rev. B **99**, 085103 (2019).
[15] M. A. McGuire, J. Yan, P. Lampen-Kelley, A. F. May, V. R. Cooper, L. Lindsay, A. Puretzky, L. Liang, S. KC, E. Cakmak, S. Calder, and B. C. Sales, Phys. Rev. Mater. **1**, 064001 (2017).
[16] H. Gretarsson, N. H. Sung, M. Höppner, B. J. Kim, B. Keimer, and M. Le Tacon, Phys. Rev. Lett. **116**, 136401 (2016).